ResearchGate

See discussions, stats, and author profiles for this publication at: https://www.researchgate.net/publication/231411998

Formation of charged silver clusters and their reversible silver ion desorption in zeolite A

ARTICLE *in* THE JOURNAL OF PHYSICAL CHEMISTRY · MAY 1986

DOI: 10.1021/j100401a027

CITATIONS
38

READS
25

3 AUTHORS, INCLUDING:

John Texter
Eastern Michigan University
232 PUBLICATIONS **2,166** CITATIONS

SEE PROFILE

Available from: John Texter
Retrieved on: 20 January 2016

Formation of Charged Silver Clusters and Their Reversible Silver Ion Desorption in Zeolite A†

John Texter,*‡

Department of Chemistry, SUNY Binghamton, Binghamton, New York 13901

Richard Kellerman,§ and Thomas Gonsiorowski⊥

Webster Research Center, Xerox Corporation, Webster, New York 14580 *(Received: July 22, 1985; In Final Form: October 28, 1985)*

Optical absorption, mass spectroscopy, magnetic susceptibility, electron spin resonance, and gas adsorption studies of the activated dehydration of silver-exchanged zeolite A show that principally diamagnetic silver clusters are formed by the activated extraction of oxygen from (oxidation of) the zeolite lattice. This oxidation is formally two-electron and, coupled with intrazeolitic silver ion mobility, can account for the concerted reduction of *pairs* of silver ions without the formation of stable paramagnetic clusters. The predominant charged cluster (B) formed in the sodalite unit has a low-energy absorption band centered at 2.72 eV and a higher lying excitation at 3.8–3.9 eV. The nuclearity of this cluster is uncertain, although it is ≥6 and ≤14. Another cluster (C) appears to coexist with cluster B and has excitations at 3.5–3.6, 4.1–4.2, and 4.9–5 eV. Sorption of olefins induces the competitive and reversible desorption of silver ions from cluster B and leads to the formation of C. Three distinct intermediates (absorption maxima at 2.9, 3.1, and 3.3 eV) have been identified during silver ion desorption from cluster B. Another intermediate (cluster A; band maximum at 3–3.1 eV) has also been identified en route to the formation of cluster B. A superposition of this 3–3.1-eV intermediate absorption of cluster A with the 2.72-eV absorption of cluster B gives the so-called yellow form of silver zeolite A. This yellow color had previously been assigned to linear and doubly charged (paramagnetic) silver trimers trapped in the sodalite unit by Gellens et al.

Introduction

The optical absorption of *neutral* Ag_n ($n < 10$) species isolated in various matrices has been studied extensively,[1-8] and, for n = 1–6, absorption spectra have been tentatively characterized. Optical absorption data for *charged* silver clusters, on the other hand, are sparse. The existence of Ag_{n+1}^+ has been postulated to explain features in the UV spectrum of γ-irradiated silver-containing sulfuric acid glasses.[9] UV bands have been tentatively assigned to Ag_2^+ and Ag_3^+, and to Ag_4^{2+} produced in aqueous solution (by γ and pulse radiolysis).[10-13] A UV absorption band of Ag_4^{3+} in aqueous and ethanol solutions was reported recently, and this observation has been corroborated by ESR measurements.[14] It has been suggested that color centers in variously reduced silver-containing zeolites[15] are Ag_n^{m+} species.[16,17] Further work with zeolite A has suggested that these centers correspond to Ag_3^{2+} species or interacting Ag_3^{2+} species.[18] Optical features in the UV spectrum of silver-containing Y zeolite have been assigned to Ag_2^+ and Ag_3^{2+} species.[19,20]

Other evidence suggests that silver has a remarkable tendency to form charged clusters under a wide range of conditions. A partial list of such species includes Ag^{2+}, Ag_3^{2+}, and Ag_4^{3+} in aqueous glasses (identified by their ESR spectra),[21,22] Ag_{12}^{6+} and Ag_{14}^{8+} in anhydrous zeolite A (inferred from single-crystal X-ray diffraction data),[23-26] Ag_6^{m+} (m = 1, 3, or 5) in hydrogen-reduced zeolite A (inferred from ESR measurements),[27] Ag_3^{2+} and Ag_4^{3+} in anhydrous A and Y zeolites, respectively (inferred from hydrogen sorption data),[16,17] and linear Ag_3^{m+} clusters and Ag_6^{m+} clusters in dehydrated A, X, and Y zeolites (inferred from optical reflectance and powder X-ray diffraction data).[18,28,29] Octahedral Ag_6 clusters (formal oxidation state not specified) have been identified in the mineral boleite,[30] and octahedral Ag_6^{4+} clusters have been resolved in the semiconductor $Ag_6Ge_{10}P_{12}$.[31] The sequential addition of interstitial silver ions and photoelectrons to form neutral, positively charged, and negatively charged clusters is an important basis for the formation of latent image in silver halide microcrystals.[32-38]

† Presented in part at the 57th Colloid and Surface Science Symposium, June 12–15, 1983, University of Toronto.

‡ Present address: Research Laboratories, Eastman Kodak Company, Rochester, NY 14650.

§ Present address: Nielsen-Kellerman Company, 201 East 10th Street, Marcus Hook, PA 19063.

⊥ Present address: Adaptive Optics Associates, 54 Cambridge Park Drive, Cambridge, MA 02140.

(1) Schulze, W.; Becker, H. U.; Abe, H. *Chem. Phys.* **1978**, *35*, 177.
(2) Ozin, G. A.; Huber, H. *Inorg. Chem.* **1978**, *17*, 155.
(3) Ozin, G. A. *Faraday Symp. Chem. Soc.* 1980, *14*, 7.
(4) Schulze, W.; Abe, H. *Faraday Symp. Chem. Soc.* **1980**, *14*, 87.
(5) Kellerman, R.; Texter, J. *J. Chem. Phys.* **1979**, *70*, 1562.
(6) Huber, H.; Mackenzie, P.; Ozin, G. A. *J. Am. Chem. Soc.* **1980**, *102*, 1548.
(7) Mitchell, S. A.; Farrell, J.; Kenney-Wallace, G. A.; Ozin, G. A. *J. Am. Chem. Soc.* **1980**, *102*, 7702.
(8) Welker, T.; Martin, T. P. *J. Chem. Phys.* **1979**, *70*, 5683.
(9) Brown, D. H.; Dainton, F. S. *Trans. Faraday Soc.* **1966**, *62*, 1139.
(10) Pukies, J.; Roebke, W.; Henglein, A. *Ber. Bunsenges. Phys. Chem.* **1968**, *72*, 842.
(11) Henglein, A. *Ber. Bunsenges. Phys. Chem.* **1977**, *81*, 556.
(12) Tausch-Treml, R.; Henglein, A.; Lilie, J. *Ber. Bunsenges. Phys. Chem.* **1978**, *82*, 1335.
(13) Henglein, A; Tausch-Treml, R. *J. Colloid Interface Sci.* **1981**, *80*, 84.
(14) Stevens, A. D.; Symons, M. C. R. *Chem. Phys. Lett.* **1984**, *109*, 514.
(15) Ralek, M.; Jiru, P.; Grubner, O.; Beyer, H. *Collect. Czech. Chem. Commun.* **1962**, *27*, 142.
(16) Beyer, H.; Jacobs, P. A.; Uytterhoeven, J. B. *J. Chem. Soc., Faraday Trans. 1* **1976**, *72*, 674.
(17) Jacobs, P. A.; Uytterhoeven, J. B.; Beyer, H. K. *J. Chem. Soc., Faraday Trans. 1* **1979**, *75*, 56.
(18) Gellens, L. R.; Mortier, W. J.; Schoonheydt, R. A.; Uytterhoeven, J. B. *J. Phys. Chem.* **1981**, *85*, 2783.
(19) Ozin, G. A.; Hugues, F. *J. Phys. Chem.* **1983**, *87*, 94.
(20) Ozin, G. A.; Hugues, F.; Mattar, S. M.; McIntosh, D. F. *J. Phys. Chem.* **1983**, *87*, 3445.
(21) Brown, D. R.; Findley, T. J. V.; Symons, M. C. R. *J. Chem. Soc., Faraday Trans. 1* **1976**, *72*, 1792.
(22) Forbes, C. E.; Symons, M. C. R. *Mol. Phys.* **1962**, *27*, 467.
(23) Kim, Y.; Seff, J. *J. Am. Chem. Soc.* **1977**, *99*, 7055.
(24) Kim, Y.; Seff, J. *J. Am. Chem. Soc.* **1978**, *100*, 175.
(25) Kim, Y.; Seff, K. *J. Am. Chem. Soc.* **1978**, *100*, 6989.
(26) Kim, Y.; Seff, K. *J. Phys. Chem.* **1978**, *82*, 1307.
(27) Hermerschmidt, D.; Haul, R. *Ber. Bunsenges. Phys. Chem.* **1980**, *84*, 902.
(28) Gellens, L. R.; Mortier, W. J.; Uytterhoeven, J. B. *Zeolites* **1981**, *1*, 11.
(29) Gellens, L. R.; Mortier, W. J.; Uytterhoeven, J. B. *Zeolites* **1981**, *1*, 85.
(30) Rouse, R. C. *J. Solid State Chem.* **1973**, *6*, 86.

0022-3654/86/2090-2118$01.50/0 © 1986 American Chemical Society

We present here an optical absorption study of the formation of silver clusters in zeolite A. The stepwise formation of clusters under conditions of vacuum dehydration and dehydration in a purging stream of oxygen is examined. The sorption of olefins induces dramatic optical changes, which are reversible and can be interpreted in terms of reversible silver ion desorption from some of the clusters.

Experimental Section

Ion Exchange. Binder-free zeolite A in the sodium form (Na_{12}–A) was obtained from the Linde Division of Union Carbide Corp. Samples were pretreated in dilute NaOH (pH 11.5) at 80 °C, filtered, and equilibrated at 50% relative humidity over saturated $Ca(NO_3)_2$. Silver ion exchanges were carried out in the dark, and hydrated exchanged samples were stored in the dark. Samples (5–15 g) for Ag^+ exchange [pseudocell formula, $Na_{12}(AlO_2)_{12}(SiO_2)_{12}\cdot 27H_2O$; formula weight, 2190 g/mol] were slurried in 200–500 mL of deionized water at room temperature, and the pH was adjusted to 7 with dilute aqueous HNO_3. Aqueous $AgNO_3$ (60 mL) containing 1 equiv of silver per pseudocell was then added to the slurry with stirring. After equilibration for 1 h, these Ag_1–A samples were filtered, washed with deionized water, and stored at 50% relative humidity.

Optical Spectroscopy. Diffuse reflectance spectra[39,40] were recorded on a Cary 14R spectrophotometer equipped with a digital interface. Disks (0.5-in. thick) of compacted Halon G-50 were used as reflectance reference standards.[41] Visible and UV spectra (8500–1900 Å) were measured in the nondispersed illumination mode with a 150-W Xe lamp as the source and a Hamamatsu R927 photomultiplier tube as the detector. The measured diffuse reflectance R_∞ values were transformed to give the remission values $F(R_\infty) = (1 - R_\infty)/(2R_\infty)$, which yield spectra equivalent to absorption spectra.[42] Room-temperature spectra were recorded with the samples in diffuse-reflectance cells 5-mm deep with an optical window of 1-mm-thick Infrasil.

Dehydration, Gas Adsorption, and Desorption. High-vacuum manifolds were used for all sample treatments. Demountable cell assemblies were used for in situ treatments of samples in spectroscopic cells. Gravimetric gas adsorption was measured with a Cahn 1000 vacuum microbalance. Gas effluent accompanying activated dehydration was analyzed on a UTI 100C quadrupole residual gas analyzer modified with an automatic peak-to-peak switching device. Volumetric gas adsorption measurements were made at room temperature.

Magnetic Measurements. Samples for electron spin resonance measurements were activated and treated in vacuum-demountable flask/ESR-tube assemblies. After sample preparation, the assembly was backfilled with He gas (to facilitate thermal equilibration), the sample was transferred to the ESR tube, and the tube was removed by using a glass pull-off. ESR spectra were recorded with a Varian 9-in. field-controlled magnet and X-band radiation. Magnetic susceptibility was measured with a Gouy balance constructed from a Cahn 1000 vacuum microbalance and a Varian 4-in. current-controlled magnet. The field was monitored with a Hall-effect magnetometer. Temperature was controlled with a liquid-nitrogen heat exchanger and a heater in a closed loop.

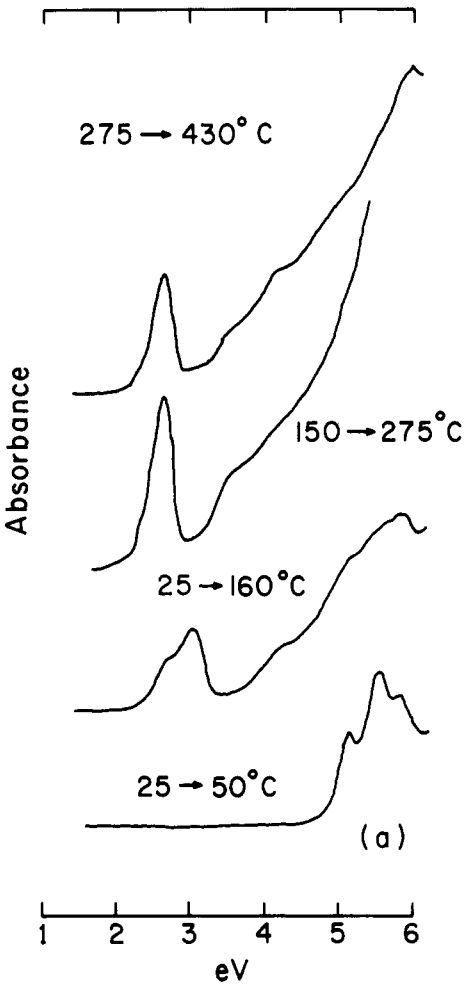

Figure 1. Diffuse-reflectance spectra of an Ag_1–A sample subjected to thermal activation in vacuo. Spectra were measured at 25 °C; activations were done in vacuo at background pressures of 10–20 μm. Activations: 25 → 50 °C curve, 25 °C for 24 h followed by 50 °C for 18 h; 25 → 160 °C curve, linear ramp from 25 to 160 °C over 16 h; 150 → 275 °C curve, linear ramp from 150 to 275 °C over 16 h; 275 → 430 °C curve, linear ramp from 275 to 430 °C over 16 h.

Results

Vacuum and Oxygen Activation. Figure 1 shows optical absorption (transformed diffuse reflectance) spectra (measured at 25 °C) of an Ag_1–A sample activated in vacuo. The initial curve (25 → 50 °C) was obtained by evacuating the sample at 25 °C for ~24 h and then evacuating at 50 °C for 18 h. The 5–6-eV multiplet in this curve corresponds to the $(4d^95s)\ ^1D \leftarrow (4d^{10})\ ^1S$ excitation of trigonally coordinated Ag^+. This multiplet has been discussed extensively elsewhere.[43] This sample was the starting point for our study of the production of charged silver clusters in zeolite A. This low-temperature (25–50 °C) vacuum activation gives white samples with 5–7 water molecules per pesudocell (as determined gravimetrically in vacuo).

The other curves in Figure 1 were measured (at 25 °C) after 16-h (linear) ramped vacuum activations of 25 → 160 °C, 150 → 275 °C, and 275 → 430 °C. A separate temperature program (50 → 100 °C, 100 → 200 °C, 200 → 300 °C; ramped at 7 °C/h and held at upper limit for 18 h) yielded essentially identical optical features. Less than 0.1 water molecule per pesudocell remained in these samples after the highest activations. An identical sequence of optical features was generated by a thermal activation program (19 h at 25 °C, 25 → 100 °C, 100 → 235 °C, 235 → 300 °C; ramped at 7 °C/h and held at upper limit for 18 h), where the Ag_1–A sample was subjected to a flowing stream of oxygen (at atmospheric pressure).

(31) Schnering, H. G.; Hausler, K.-G. *Rev. Chim. Miner.* **1976**, *13*, 71.
(32) Gurney, R. W.; Mott, N. F. *Proc. R. Soc. London, Ser. A* **1938**, *A164*, 151.
(33) Matejec, R. *Z. Phys.* **1957**, *148*, 454.
(34) Hamilton, J. F. *Photogr. Sci. Eng.* **1979**, *14*, 102.
(35) Hamilton, J. F. *Prog. Solid State Chem.* **1973**, *8*, 167.
(36) Mitchell, J. W. *Photogr. Sci. Eng.* **1979**, *23*, 1.
(37) Mitchell, J. W. *Photogr. Sci. Eng.* **1981**, *25*, 170.
(38) Sahyun, M. R. V. *Stud. Surf. Sci. Catal.* **1980**, *4*, 379.
(39) Kortum, G. *Reflectance Spectroscopy*; Springer-Verlag: New York, 1969.
(40) Delgass, N.; Haller, G.; Kellerman, R.; Lunsford, J. *Spectroscopic Techniques in Heterogeneous Catalysis Research*; Academic: New York, 1979.
(41) Grum, F.; Salzman, M. *Proceedings of the Eighteenth International Committee on Illumination, London, 1975*; CIE Publication No. 36, 1976; pp 75–77.
(42) Klier, K. *J. Opt. Soc. Am.* **1972**, *62*, 882.
(43) Texter, J.; Gonsiorowski, T.; Kellerman, R. *Phys. Rev. B* **1981**, *23*, 4407.

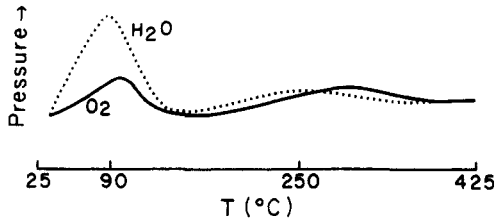

Figure 2. Quadrupole residual gas pressures evolved in the thermal vacuum activation of hydrated Ag_1–A; linear temperature ramp (25–420 °C), 40 h.

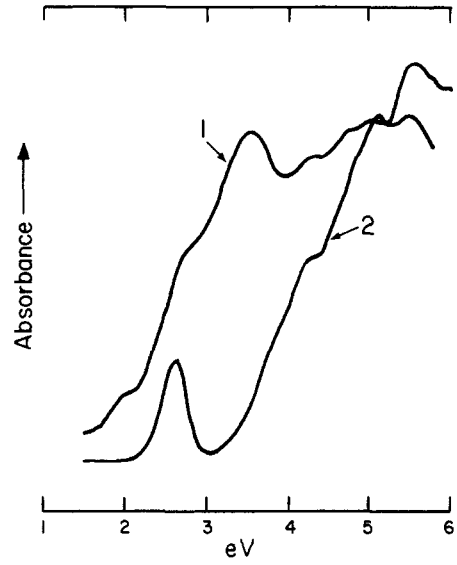

Figure 3. Diffuse-reflectance spectra of an Ag_1–A sample after activation (curve 1) as in Figure 2; (curve 2) same sample after treatment with oxygen (500 torr for 1 h at 350 °C).

These separate thermal vacuum-activation programs produced similar optical features. The first significant feature is the *intermediate* band at 3.05–3.1 eV evident in the 25 → 160 °C curve. This feature emanates from a cluster we designate as A. These samples are pale yellow. A second feature is a pronounced shoulder at ~2.7 eV. Lower intensity shoulders at 4.2 eV and remnants of the 5–6-eV Ag^+ multiplet are evident on the rising higher energy continuum. Further activation, shown by the 150 → 275 °C curve, caused the 2.7-eV band to grow and the 3.1-eV band to disappear. These samples are salmon-colored. The 4.2-eV shoulder is still evident. However, an additional shoulder at 3.5 eV has appeared. Additional activation produces no new features.

The *intermediate* (cluster A) that gives the 3.1-eV (yellow) band appears before the species that gives the 2.7-eV (salmon) peak. This second band has a peak at ~2.72 eV, with a shoulder at 2.38 eV. We designate as cluster B the species that gives this 2.7-eV band.

We studied the gaseous evolution during the vacuum activation of an Ag_1–A sample, using a quadrupole residual gas analyzer. A 4-g sample of Ag_1–A hydrate was first evacuated at 25 °C for 18 h. Such activation caused the loss of 11.2 ± 1.4 water molecules per pseudocell. A 40-h linear temperature ramp (25–425 °C) was then applied to the sample, and the residual water and oxygen evolution were followed with the gas analyzer. Figure 2 shows the analyzer response for water and oxygen evolution. Two distinct pressure waves resulted, a major wave at 90–100 °C and a second wave peaking at ~250 °C. The oxygen waves *lag* the water waves. The relative oxygen-to-water response in the higher-temperature region is about 3 times higher than in the major 90–100 °C wave.

The absorption spectrum of the Ag_1–A sample produced by this 25–425 °C ramp activation is shown in Figure 3 (curve 1). This spectrum shows the importance of the *rate* and detailed history of activation in controlling the distribution of types of silver clusters. Distinct peaks are observed at 3.5, 4.3, 5, and 5.5 eV, with shoulders at 2 and 2.7 eV. Subsequent treatment of this

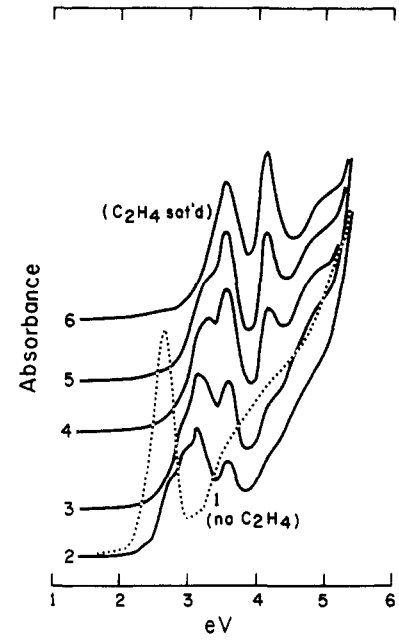

Figure 4. Diffuse-reflectance spectra showing optical changes in a vacuum- and oxygen-activated Ag_1–A sample (curve 1) as it is saturated with ethylene. Spectra were recorded at 25 °C. Curves 2–6 correspond to ethylene loadings of 1.5, 2, 3, 4, and 5.7 molecules per pseudocell, respectively.

sample for 1 h at 350 °C with oxygen at 500 torr produced the dramatic change shown in curve 2 of Figure 3. The 2- and 3.5-eV features of curve 1 are obliterated by this treatment, and the 2.7-eV peak, apparently highly resistant to activated oxidation, remains.

An identically prepared Ag_1–A (salmon) sample was examined at 15 K for an ESR signal. The spectrum showed that the only apparent absorptions (at 1540 and 3270 G) are also present in a vacuum-dehydrated Na_{12}–A sample. These absorptions are due to (lattice) substitutional Fe^{3+} arising from Fe_2O_3 impurities in the alumina used in preparing the zeolite.[44-50] This lack of an ESR signal attributable to silver species is not conclusive evidence for the absence of paramagnetic silver species. Thus we repeated these sample preparations and measured volume magnetic susceptibility (10–330 K) on a Gouy balance. The inverse temperature dependence of the net susceptibilities gave Curie temperatures of 1.32×10^{-5} and 1.39×10^{-5} K, respectively, for the Ag_1–A and Na_{12}–A samples. The essentially identical paramagnetism measured in these two samples (~0.6 Bohr magnetons per pseudocell) can be attributed to Fe^{3+} impurities. We conclude that there is no significant population of paramagnetic silver species in the Ag_1–A sample.

Olefin Adsorption. The species that gives the 2.7-eV band is resistant to activated oxidation. In this section we examine the interactions of ethylene, *cis*-butene, and *trans*-butene with this species. The spectra in Figure 4 show how a vacuum- and oxygen-pretreated Ag_1–A sample (curve 1) is gradually transformed by increasing doses of ethylene at room temperature. Samples were equilibrated for 2–24 h between doses. Curves 2–6 correspond to ethylene loadings of 1.5, 2, 3, 4, and 5.7 (saturated) molecules per pesudocell. The ethylene-saturated sample was yellow and gave distinct absorption peaks at 3.6, 4.2, and 4.9 eV (curve 6). Of particular interest are the *intermediate* optical features that appear during this sequential dosing at 2.9, 3.15, and 3.3 eV as the 2.7-eV peak gradually vanishes. The 3.5–5-eV rising continuum of curve 1 is transformed as well by this ethylene

(44) Jones, S. *J. Electrochem. Soc.* **1949**, *95*, 295.
(45) Hummel, F. A.; Sastry, B. S. R.; Wotring, D. *J. Am. Ceram. Soc.* **1959**, *41*, 88.
(46) Dvir, M.; Low, W. *Phys. Rev.* **1969**, *119*, 1587.
(47) Mochel, V. D. *J. Electrochem. Soc.* **1966**, *113*, 398.
(48) Pott, G. T.; McNicol, B. D. *Chem. Phys. Lett.* **1970**, *6*, 623.
(49) Melamed, N. T.; Viccaro, P. J.; Artman, J. O.; Barros, F. de S. *J. Lumin.* **1970**, *1,2*, 348.
(50) Pott, G. T.; McNicol, B. D. *Chem. Phys. Lett.* **1971**, *12*, 62.

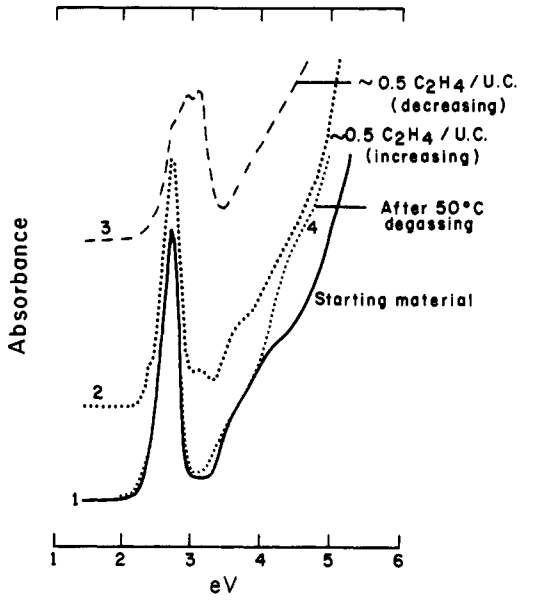

Figure 5. Diffuse-reflectance spectra (25 °C) showing reversibility of the optical effects of Figure 4 that accompany ethylene sorption and desorption. Only slight vacuum activation (50 °C) is required to completely restore the 2.7-eV peak.

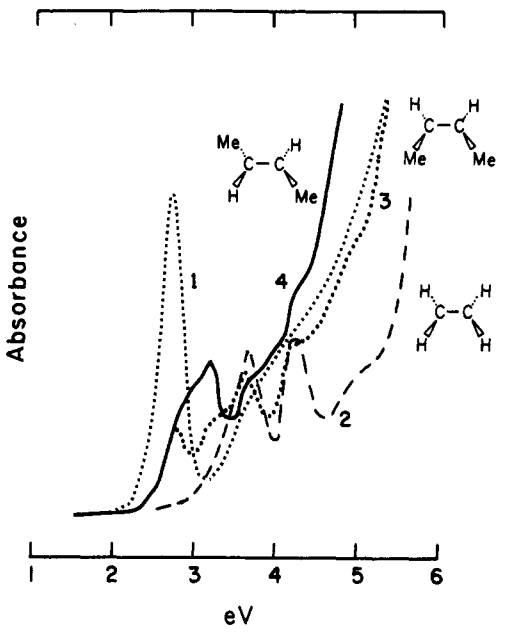

Figure 6. Diffuse-reflectance spectra (25 °C) showing comparable effects of *cis*-butene and *trans*-butene sorption on the 2.7-eV optical feature. Gas sorption was done at 25 °C. Curve 2 corresponds to curve 6 of Figure 4 (ethylene saturated); curve 3, similar sample saturated with *cis*-butene; curve 4, similar sample saturated with *trans*-butene. Curve 1 was obtained by 100 °C vacuum activation of either of the butene-saturated samples.

sorption. This transformation is most evident as a distinct loss of absorption intensity at 3.8–3.9 eV. The optical effects of this ethylene sorption are reversible, with hysteresis (see Figure 5). This reversibility is nearly total at room temperature. Curve 3 in Figure 5 corresponds to an ethylene-saturated sample that had been exhaustively degassed in vacuo at room temperature. About 0.5 ethylene per pseudocell remained in this sample, and the intermediate 2.9- and 3.15-eV features are evident. Increasing the temperature during evacuation to 50 °C completely desorbed the ethylene, and the 2.7-eV band was completely restored (curve 4 in Figure 5).

Saturation sorption by *cis*-butene and *trans*-butene produced optical effects similar to those produced by ethylene sorption (Figure 6). Saturation with *cis*-butene (curve 3) produced optical features that nearly matched those resulting from ethylene saturation (curve 2). An intermediate feature at 3.3 eV and a much reduced 2.7-eV peak are still evident (curve 3). Saturation with the more sterically hindered *trans*-butene (curve 4) also results in budding components at 3.6 and 4.2 eV. However, the optical transformation largely stopped at the 2.9- and 3.15-eV intermediate stage. Removal of these butenes at 100 °C in vacuo restored the original 2.7-eV feature (curve 1).

Discussion

Reduction Mechanisms. Autoreduction mechanisms of silver zeolites have been studied in a number of laboratories.[23-29,51-58] These mechanisms have been postulated to involve the oxidation of water or the extraction and subsequent liberation of oxygen from the zeolite framework. Photochemical pathways involve the oxidation of water and produce hydroxylated zeolite sites (ZOH).[51,53] At higher temperatures these sites can be oxidized by elemental silver to release molecular hydrogen.[51,53] Thermal pathways have been postulated to proceed by extraction of oxygen from the framework and the production of Lewis-acid sites (Z^+).[17,18] Gellens et al.[18] have depicted this pathway in terms of the following stoichiometry, where ZO^- represents a cation binding site:

$$2(Ag^+ZO^-) \rightarrow {}^1/_2O_2 + 2Ag^0 + Z^+ + ZO^-$$

Such a pathway involves oxygen extraction without the formation of hydroxyls. Our residual-gas-analyzer data of Figure 2 are consistent with this pathway, since it illustrates the thermal evolution of oxygen. We could also observe the loss of water by monitoring the decrease of the $\nu_3 + \delta$ combination band of water in the near-infrared (NIR).[59-61] We could not detect the formation of hydroxyls in the 2ν overtone region in the NIR. These vibrational data are also consistent with the above stoichiometry.

Mechanistically, the above stoichiometry is likely produced by several sequential steps. We would like to focus on several possibilities for the basic steps in this process, since much of the literature on silver zeolites concerns the formation of charged clusters with a single unpaired spin. The existence of such clusters under the autoreduction conditions reported here and elsewhere necessitates the formation of isolated silver atoms that cannot dimerize before adsorbing silver ions. The above stoichiometry is somewhat misleading from a redox point of view in that one of the sites is superfluous and the oxidation half-cell formally involves a single zeolite site:

$$ZO^- \rightarrow {}^1/_2O_2 + Z^+ + 2e^-$$

When this half-cell is considered, the basic reduction mechanism would appear to be a two-electron process centered on a single zeolite site. If an Ag^+ ion were initially reduced to the atom, subsequent reduction may produce the Ag^- species. Ionic conductivities in silver zeolites are too large to measure conveniently.[62] Rapid complexation with a mobile Ag^+ would give a metastable silver dimer that is not paramagnetic. Subsequent Ag^+ adsorption would not change the net spin. Alternatively, if an Ag^+ ion or

(51) Jacobs, P. A.; Uytterhoeven, J. B.; Beyer, H. K. *J. Chem. Soc., Chem. Commun.* **1977**, 128.
(52) Jacobs, P. A.; Linart, J.-P.; Nijs, H.; Uytterhoeven, J. B.; Beyer, H. K. *J. Chem. Soc., Faraday Trans. 1* **1977**, *73*, 1745.
(53) Leutwyler, S.; Schumacher, E. *Chimia* **1977**, *31*, 475.
(54) Tsutsumi, K.; Takahashi, H. *Bull. Chem. Soc. Jpn.* **1972**, *45*, 2332.
(55) Ozin, G. A.; Baker, M. D.; Parnis, J. M. *Angew. Chem. Suppl.* **1983**, *1075*.
(56) Ozin, G. A.; Baker, M. D.; Godber, J. *J. Phys. Chem.* **1984**, *88*, 4902.
(57) Baker, M. D.; Ozin, G. A.; Godber, J. *J. Phys. Chem.* **1985**, *89*, 305.
(58) Baker, M. D.; Godber, J.; Ozin, G. A. *J. Phys. Chem.* **1985**, *89*, 4658.
(59) Klier, K.; Shen, J. H.; Zettlemoyer, A. C. *J. Phys. Chem.* **1973**, *77*, 1458.
(60) Texter, J.; Strome, D. H.; Herman, R. G.; Klier, K. *J. Phys. Chem.* **1977**, *81*, 333.
(61) Texter, J.; Klier, K.; Zettlemoyer, A. C. *Prog. Surf. Membr. Sci.* **1978**, *12*, 327.
(62) Huggins, R. A., private communication made at the International Conference on Fast Ion Transport in Solids, Lake Geneva, WI, May 21–25, 1979.

two adsorbed to the atom before the second electron was released from the lattice, the Ag_2^+ or Ag_3^+ species could be converted rapidly to the respective neutral dimer or Ag_3^+ species.

An alternative view[17] of this oxidation half-cell has been given in terms equivalent to the following:

$$ZO^- \rightarrow O^- + Z^+ + e^-$$

$$O^- \rightarrow {}^1/_2O_2 + e^-$$

The first of these oxidations reduces an Ag^+ near the ZO^- site. The second oxidation was considered to reduce an Ag^+ ion at another ZO^- site. For these silver atoms to remain separate, paramagnetic species, the seond-stage reduction would require the diffusion of O^- away from the first, now positively charged, site.

We cannot experimentally resolve whether this autoreduction–nucleation, in its embryonic stage, gives separate or dimerized silver atoms. However, the considerations raised above can be supplemented by the theoretical studies of Mitchell[63] and of Baetzold and Hamilton[64–67] on the electronic structure and stability of small neutral and charged silver clusters. Neutral clusters containing an even number of atoms are more stable than odd-numbered clusters. These odd-numbered clusters have significantly higher electron affinities than the even-numbered ones.

Formation of Charged Clusters. Dehydration in vacuo (Figure 1) and under a purging oxygen stream gives optically identical silver-cluster-containing Ag–A samples, when dehydration is carried out *slowly* and in *gradual stages*. These same dehydration procedures show that the yellow samples contain at least two (clusters A and B) types of clusters (2.72- and 3.1-eV absorptions). Gellens et al.[18] produced yellow $Ag_{2.4}$–A and Ag_{12}–A samples by dehydrating in vacuo at 105 °C for 2 days. They reported a well-resolved absorption band at 2.8–2.9 eV and broad higher energy features at 4–4.2 and 4.6–4.9 eV. The published spectrum of their yellow Ag_{12}–A sample is similar to the 100 °C curve of Figure 1. They assigned this yellow absorption band to linear Ag_3^{2+} species contained in the sodalite cavity on the basis of powder X-ray diffraction structural refinements and extended Hückel molecular orbital calculations. Global geometries were not optimized in these calculations, however. Hückel molecular orbital theory predicts that the (D_{3h}) triangular geometry is more stable than the linear form in free Ag_3^{2+},[68] as also do ab initio self-consistent field and configuration interaction methods.[69]

Gellens et al.[18] found that subsequent dehydration at 243 °C produced brick-red $Ag_{2.4}$–A and Ag_{12}–A samples with optical features at 2.4–2.6 and 3.4–3.6 eV. They assigned these optical features to a pair of interacting Ag_3^{2+} species in the sodalite cage. The published spectrum of their brick-red Ag_{12}–A sample has little similarity to the spectra of salmon-colored samples (dehydrated at 300 °C) of Figure 1. It does, however, qualitatively coincide with curve 1 of Figure 3, which was obtained by a continuously ramped temperature-dehydration program, in contrast to the slow stepped procedure of Figure 1. Figure 3 also shows that the 2.7-eV peak is recovered by treatment with oxygen at 350 °C. It is not possible to determine whether the 2.7-eV feature is present before this activated-oxygen treatment and is obscured by the absorptions of the other clusters formed. It is, however, very stable to activated oxidation.

The dominant feature at 3.5 eV (354 nm) in curve 1 of Figure 3 and the low-energy feature at 2 eV (625 nm) may be due to neutral Ag_n clusters (n = 5–10). This assignment is based solely on comparisons with spectra of neutral silver clusters obtained in rare-gas,[1,2] zeolite Y,[5] and paraffin[6] matrices. Curve 1 of Figure 3 corresponds qualitatively to the curves from brick-red zeolite samples prepared by Gellens et al., which they interpreted as having charged-hextuplet clusters or pairs of interacting Ag_3^{2+} clusters in the sodalite cage. We cannot interpret the many peaks and shoulders in Figure 3 (curve 1) in terms other than the presence of several neutral and possibly charged clusters.

The optical features of the yellow intermediate and the salmon-colored samples (clusters A and B) cannot be satisfactorily correlated with any published spectra of neutral silver clusters. However, the magnetic data show conclusively that no detectable paramagnetic silver clusters are present in samples that have been treated to give the 2.7-eV band.

These spectra (Figure 1) show the existence of at least two types of silver clusters in yellow samples, in addition to trigonally coordinated Ag^+ ions. We believe that multiple types of clusters are also present in the salmon-colored samples. A consideration of the earlier discussion of autoreduction suggests to us that the basic nuclearity during cluster formation is two. Cluster growth, at all stages, can occur by adsorption of Ag^+ ions as a result of activated ionic diffusion. Further two-electron reductions of charged clusters could occur by the same basic autoreduction mechanism. Such growth would require that the redox potential near nuclei is more favorable than that at isolated (Ag^+ZO^-) sites. Independent evidence shows that the extent of autoreduction in Ag–A samples, under fixed activation conditions, increases with increasing Ag^+ loading of the zeolite.[17]

Cluster Location. We believe that cluster B (and the precursor A) is located in the sodalite unit. This belief is based on the preponderance of X-ray data reported by Kim and Seff[23–26] and by Gellens et al.[18] Although sample preparations and the assignments of cluster structures reported by these groups differ, the locations have been uniformly intrasodalitic.

Chemical evidence also suggests that B is located in the sodalite unit. Curve 2 of Figure 3 shows that B is highly resistant to activated oxidation, and the sodalite unit would be expected to provide a high degree of steric stabilization. Clusters formed during the relatively rapid activation, illustrated in curve 1 of Figure 3, are probably located in the large α cage or may even in part be extrazeolitic. They are easily oxidized in an activated oxygen environment.

The hysteresis in ethylene sorption, illustrated in Figure 5, also is consistent with an intrasodalitic location for cluster B. The 50 °C activation required to complete the ethylene desorption is 15 °C lower than that found earlier[43] to be necessary for the removal of ethylene from Ag^+ ions trigonally coordinated in the α cage. These ions migrate back through the hexagonal windows into the sodalite unit when not bound to ethylene.

Reversible Ag^+ Desorption from Cluster B. Kim and Seff[24] have shown by single-crystal X-ray diffraction that ethylene forms a trigonal complex with Ag^+ in Ag_{12}–A samples that have been vacuum dehydrated under mild conditions. The Ag^+ ions are trigonally coordinated to three oxygens in the hexagonal six-rings, and ethylene molecules in the α cage are bound to Ag^+ ions along the principal C_{3v} symmetry axis. This bonding occurs as a result of overlap between the empty Ag^+ 5s and filled ethylene π orbitals and so-called back-donation between filled Ag^+ $4d_{xz}$, $4d_{yz}$ and empty ethylene π^* orbitals, as has been described by Dewar.[70] We showed earlier[43] that the expected effects of such bonding on the UV absorption band corresponding to the 5s ← 4d excitation of Ag^+ in $Ag_{0.1}$–A are in fact observed.

This complexation between ethylene and Ag^+ forms a chemical basis for our model of reversible Ag^+ desorption from cluster B. This basis involves competitive equilibria between Ag^+–ethylene and Ag^+–cluster binding. The olefin adsorption and desorption data of Figures 4–6 show conclusively that the effects of olefin sorption are reversible. The sequence of three intermediate absorption bands at 2.9, 3.1, and 3.3 eV (Figure 4) corresponds, we believe, to the stepwise desorption of Ag^+ ions. The initial Ag^+ desorption occurs most readily with the most highly favored equilibria (2.9- and 3.1-eV absorption peaks), and the formation and destruction of the intermediate cluster with the 3.3-eV absorption occurs only at the highest intrazeolitic ethylene activities (curves 4–6 in Figure 4). A mechanism not involving specific Ag^+

(63) Mitchell, J. W. *Photogr. Sci. Eng.* **1978**, *22*, 1.
(64) Hamilton, J. F.; Baetzold, R. C. *Science* **1979**, *205*, 1213.
(65) Baetzold, R. C. *J. Chem. Phys.* **1971**, *55*, 4355.
(66) Baetzold, R. C. *J. Chem. Phys.* **1971**, *55*, 4363.
(67) Baetzold, R. C. *J. Chem. Phys.* **1978**, *68*, 555.
(68) Baetzold, R. C., private communication.
(69) Basch, H. *J. Am. Chem. Soc.* **1980**, *103*, 4657.
(70) Dewar, M. J. S. *Bull. Soc. Chim. Fr.* **1951**, *18*, C71.

ion desorption, such as a local dielectric effect or a modified intrasodalitic coordination of the cluster (because of the sorbed ethylene), would be expected to produce more continuous absorption changes in the peak absorption energy.

In the context of our proposed model, the initial sorption of olefins in the α cage is not very site specific. Curve 2 of Figure 5 shows that, at an initial ethylene uptake of 0.5 molecule per pseudocell, only a few of the B clusters have been transformed. Sequentially greater effects are shown in Figure 4. Greater ethylene loadings are required to increase the concentration of π electron density near the hexagonal windows. The subsequent Ag^+ desorption occurs as the competitive olefin ligands present themselves, in a suitable orientation, at these hexagonal windows. The spectra in Figure 6 show that the extent of Ag^+ desorption decreases as the sorbed olefins become more sterically hindered in their access to the hexagonal windows (oxygen 6-rings). A considerable mixture of 2.7-, 2.9-, 3.1-, and 3.3-eV absorptions is evident (curve 4) in the sample saturated with *trans*-butene, whereas none of these absorption bands are present after saturation with ethylene (curve 2). These data are consistent with our model, wherein olefin sorption competitively removes Ag^+ ions from intrasodalitic clusters and coordinates these ions at trigonal sites in the α cage.

The bands resolved (3.5, 4.1, and 4.9 eV) after ethylene saturation are assigned to a Ag^+ ion–desorption product cluster C. Since shoulders at 3.5 and 4.1 eV are evident in the data (salmon-colored samples) of Figures 1 (275 → 430 °C curve) and 4 (curve 1), C appears to be present, to a small extent, in these samples (before ethylene sorption). These features become clearly resolved and do not shift significantly as ethylene sorption proceeds. The difference spectrum obtained by subtracting curve 2 in Figure 4 from curve 1 suggests that an additional absorption at 3.8–3.9 eV may be attributed to cluster B.

Oxidation State of Cluster B. For discussion we consider cluster B, Ag_n^{m+}, to have nuclearity n and positive charge m. The existence of three intermediates, illustrated in the olefin sorption experiments, implies that at least four Ag^+ ions can be desorbed from B. The oxidation state is therefore relatively high, and m is therefore 4 or more. This high oxidation state is consistent with the chemical resistance to further oxidation shown by B (Figure 3).

Bounds on the Nuclearity of Cluster B. The lack of detectable paramagnetism of cluster B, as shown by our ESR and bulk susceptibility experiments, implies that the difference $(n - m)$ between the total nuclearity (n) and the net positive charge (m) is *even*. A minimum value of 6 is therefore implied for n; 14 can be taken as an upper limit for n, since Kim and Seff[24] have shown that a cluster of such a size is about the largest that can be accommodated in the sodalite unit. More than a dozen clusters meeting these constraints can be envisioned; only three of these, Ag_6^{4+}, Ag_{12}^{6+}, and Ag_{14}^{8+}, have been postulated previously.

If all adsorbed Ag^+ ions are removed from cluster B after saturation with ethylene, we are faced with rationalizing these UV excitations of cluster C in terms of neutral-cluster absorptions, since those for the ethylene–Ag^+ complex lie above 6 eV.[43] The only possible candidates are the neutral dimer and tetramer, since larger clusters have absorptions below 3 eV. Monodispersed atoms and the trimer are excluded on the basis of the magnetic data. Matrix-isolation spectra of the dimer have bands at 5.5, 5, 4–4.5, and 3.1 eV.[71,72] Similar spectra of the tetramer have absorption bands at 5.5 and 3.5 eV and possibly additional bands at 4.2 and 2.8 eV.[71] Correlating these band systems with that of curve 6 in Figure 4 requires that we invoke separate matrix effects for different absorption bands to explain the different shifts. An assignment of these bands to the Ag_2 molecule is problematic because of the magnitude of the matrix effects (shifts) necessary to fit the spectrum. The two lowest energy transitions of Ag_2 are shifted up (to 3.1–3.2 eV) by 0.3 eV (lowest) and down (to 4.3 eV) by 0.3 eV (second band) relative to gas-phase transition energies when isolated in Kr or Xe matrices. These trends would have to be extended an additional 0.2–0.3 eV to fit the 3.5- and 4.1-eV features of curve 6 in Figure 4. These shifts are 0.5–0.6 eV when compared with gas-phase values. No cases have been documented that produce such shifts for neutral molecules in zeolites. The shift induced by the zeolite lattice in the lowest energy excitation multiplet of Ag^+ is comparable to a 0.5-eV shift[43] but also involves an intershell configurational excitation that is very sensitive to repulsive interactions. We therefore believe that the clusters remaining after ethylene saturation are still positively charged, where one or some of the Ag^+ ions may have significantly higher affinity for cluster association than for the available ethylene. These data do not warrant a more precise estimate of the nuclearity of cluster B.

Effects of Cluster Charge on Transition Energies. Our model for Ag^+ ion desorption from cluster B, in conjunction with the series of intermediate absorption bands shown in Figure 4, implies that the lowest observed transition energy increases as Ag^+ ions are removed from the cluster. It will be useful to compare this trend with results of theoretical studies of the optical properties of silver clusters. Transition energies estimated by a variety of quantum mechanical methods for silver clusters, containing two or three atoms and variable charge, are plentiful in the region of 2–5 eV.[73-76]

Qualitative insight into the effects of cluster charge on transition energies can be obtained from the work of Schoonheydt et al.[74] and of Ozin et al.[77] Schoonheydt et al. studied silver dimers and linear trimers encapsulated in primary hydration shells (to simulate the polarizable zeolitic framework). They found uniformly for the different geometrical models considered that the calculated lowest energy transitions increased in energy as the charge on the clusters was increased positively. Ozin et al. obtained comparable results for the linear trimer[73] and noted a similar trend in their study[77] of trigonal bypyramidal Ag_5^{q+} for $q = 0$, 2, and 4. It appears that at *constant nuclearity*, increasing charge results in increasing transition energies for the lowest allowed transitions. We would therefore expect that the lowest energy excitation for the doubly charged trimer is higher than that of the neutral species (2.8–3 eV in rare-gas matrices).[1,2] More complex considerations are necessary when both *charge and nuclearity* are changed simultaneously, as in silver ion desorption. The only model calculations available on this point are those of Schoonheydt et al.[74] Their calculated lowest energy transitions for Ag_3^{2+}, Ag_2^+, and Ag^0 were 2.78, 3.41, and 3.66 eV, respectively. For Ag_3^+ and Ag_2 they obtained transition energies of 2.25 and 2.23 eV, respectively. The trend obtained in the first of these series agrees qualitatively with our data and with our model of reversible Ag^+ desorption.

Conclusions

The predominant charged silver clusters formed in Ag–A zeolite during mild autoreduction are not paramagnetic. This finding contradicts earlier assignments of cluster structure.[18] A chemical basis for this lack of paramagnetism includes the two-electron nature of oxygen extraction from the zeolite framework. This two-electron reduction of silver ions can be concerted because of the mobility of silver ions and the higher electron affinity of silver atoms and neutral clusters of odd nuclearity. At least two, and possibly three, distinct clusters are formed during mild (low-temperature slow vacuum activation) autoreduction. The species giving the absorption bands at 2.72 and 3.8–3.9 eV can be produced by several types of activation (dehydration in vacuo, de-

(71) Mitchell, S. A.; Ozin, G. A. *J. Phys. Chem.* **1984**, *88*, 1425.
(72) Mitchell, S. A.; Kenney-Wallace, G. A.; Ozin, G. A. *J. Am. Chem. Soc.* **1981**, *103*, 6030.
(73) Ozin, G. A.; Hugues, F.; McIntosh, D. F.; Mattar, S. In *Intrazeolite Chemistry*; Stucky, G. D., Dwyer, F. G., Eds.; ACS Symp. Ser., No. 218; American Chemical Society: Washington, DC, 1983; pp 409–437.
(74) Schoonheydt, R. A.; Hall, M. B.; Lunsford, J. H. *Inorg. Chem.* **1983**, *22*, 3839.
(75) Ozin, G. A.; Huber, H.; McIntosh, D.; Mitchell, S.; Norman, Jr., J. G.; Noodleman, L. *J. Am. Chem. Soc.* **1979**, *101*, 3504.
(76) Gellens, L. R.; Mortier, W. J.; Lissillour, R.; Le Beuze, A. *J. Phys. Chem.* **1982**, *86*, 2509.
(77) Ozin, G. A.; Mattar, S. M.; McIntosh, D. F. *J. Am. Chem. Soc.* **1984**, *106*, 7765.

hydration in a stream of oxygen, oxidation after severe thermal vacuum dehydration). At least one intermediate species (cluster A, giving an absorption at 3-3.1 eV) has been identified en route to the formation of cluster B (2.72-eV absorption). This intermediate has considerable thermal stability at 50-100 °C. Earlier reports of yellow Ag-A zeolites were based on sample preparation conditions that we have shown yield mixtures of clusters. The yellow color is a result of the admixture of 2.72- and 3-3.1-eV absorption bands. Cluster B is thermally stable up to 430 °C, and this absorption imparts a salmon color to Ag-A samples when the 3-3.1-eV intermediate has been eliminated. Rapid and severe vacuum thermal activation (which generates brick-red samples) also produces samples with several types of clusters, and the presence of neutral clusters of nuclearity >6 is strongly suggested by the many low-energy absorptions. Olefin sorption experiments show that adsorbed silver ions can be competitively and reversibly desorbed from cluster B, and four stages of silver ion desorption have been identified.

Acknowledgment. We thank Prof. G. A. Ozin for making preprints available and for stimulating discussions. We also thank Prof. Ozin, Dr. R. C. Baetzold, and Prof. K. Klier for their criticisms and suggestions given during the preparation of this manuscript.

Registry No. Ag, 7440-22-4; ethene, 74-85-1; *cis*-butene, 590-18-1; *trans*-butene, 624-64-6.

Surface Properties of Poly(ethylene terephthalate) Films Modified by Far-Ultraviolet Radiation at 193 nm (Laser) and 185 nm (Low Intensity)

Sylvain Lazare*† and R. Srinivasan*

IBM Thomas J. Watson Research Center, Yorktown Heights, New York 10598 *(Received: July 29, 1985; In Final Form: January 10, 1986)*

The surfaces of poly(ethylene terephthalate) obtained by irradiation with the 193-nm pulsed radiation of the ArF excimer laser (10^7 W/cm^2) in air or the 185-nm low-intensity (2.5 mW/cm^2) radiation of the mercury lamp in a vacuum were studied and compared. The XPS analysis reveals that both are depleted in oxygen, but the efficiency of the change is intensity dependent as a result of nonlinear effects at high intensity. The pulsed radiation, which gives ablative photodecomposition when the energy of the pulse is >40 mJ/cm^2, yields a rough surface. SEM analysis shows that the roughness (i) has an amplitude which increases with the accumulation of pulses and reaches a maximum (1-2-μm spacing) at 10 pulses, and (ii) shows some periodicity. Since the chemical composition of the laser-treated surface does not vary with the accumulation of pulses, the increase in the advancing contact angle with water is interpreted as due to roughness. Labeling reactions and XPS have been used to probe the reactivity of the modified surfaces. Carboxylic acids, alcohols, and olefins were qualitatively and quantitatively probed. The laser treatment has a superior ability to create new functionalities.

Introduction

The capability of ultraviolet radiation to modify polymer surfaces by photooxidation,[1] photodegradation,[2] and photografting[3] has already been demonstrated by other groups. These studies mainly used light of wavelength greater than 200 nm that penetrates well below the surface of the polymers causing photodegradation of the bulk structure. Recently, we pointed out[4] that far-UV radiation (180 nm < λ < 200 nm), which has a small penetration depth in organic solids because of high absorption cross-section,[5] is much more adapted to surface and thin films modifications. Moreover the energy of a far-UV photon[6] (>6 eV or 138 kcal/mol) exceeds the energy of most covalent bonds in polymer chains and therefore has a high probability of photochemical bond breaking.[7] High-intensity irradiations (10^7 W/cm^2) are achieved with the pulsed output at 193 nm of an ArF excimer laser whereas low-intensity photolysis (2.5 mW/cm^2) is done with a mercury resonance lamp at a similar wavelength, i.e., 185 nm.

The superiority of lasers as light sources resides in the fact that their high intensity allows nonlinear photochemical processes to be observed in organic systems. The pulsed radiation of the excimer laser has opened up a variety of new processes which are very attractive for surface modification. The first was the ablative photodecomposition (APD) introduced in 1982.[8,9] As shown schematically in Figure 1, when a laser pulse (e.g., 193 nm of ArF excimer laser) whose fluence is above a well-defined threshold[9] falls on a polymer surface the photolyzed material is spontaneously etched away to a depth d' which is in principle less than the penetration depth d of the radiation (Figure 1). The dependence of the etch depth d' on the experimental conditions and nature of the polymer[10] as well as a theoretical description of the mechanism[11] are described in earlier publications. The process which can be seen as self-developing, dry-etching has led to many potential applications in technology[10] and microsugery.[12] Of

† Permanent address: U.A. 349 du C.N.R.S, University of Bordeaux I, 33405 Talence Cedex, France.

(1) (a) Owens, D. K. *J. Appl. Polym. Sci.* **1975**, *19*, 3315. (b) Clark, D. T.; Dilks, A. *J. Polym. Sci., Polym. Chem. Ed.* **1977**, *15*, 2321. (c) Peeling, J.; Clark, D. T. *J. Polym. Sci., Polym. Chem. Ed.* **1983**, *21*, 2047; *J. Appl. Polym. Sci.* **1981**, *26*, 3761; *Polym. Degrad. Stab.* **1980**, *3*, 97; **1981**, *3*, 177. (d) Peeling, J.; Courval, G.; Jazzar, M. S. *J. Polym. Sci., Polym. Chem. Ed.* **1984**, *22*, 419.

(2) Blais, P.; Day, M.; Wiles, D. M. *J. Appl. Polym. Sci.* **1973**, *17*, 1985.

(3) Tazuke, S.; Matoba, T.; Kimura, H.; Okada, T. *ACS Symp. Ser.* **1980**, *121*, 217.

(4) Lazare, S.; Ho, P. D.; Baker, J. M.; Srinivasan, R. *J. Am. Chem. Soc.* **1984**, *106*, 4288.

(5) These transitions can be valence bond (bonding-to-antibonding orbitals) as well as Rydberg in character.

(6) It is of practical importance to note that far-UV radiation (180 nm < λ < 200 nm) is only weakly absorbed by oxygen in air and does not require a vacuum. Quartz optical elements transmit this radiation well.

(7) Srinivasan, R.; Ors, J. A. *J. Am. Chem. Soc.* **1978**, *100*, 7089. Srinivasan, R.; Baum, T.; Ors, J. A. *Tetrahedron Lett.* **1981**, *23*, 1863.

(8) Srinivasan, R.; Mayne-Banton, V. *Appl. Phys. Lett.* **1982**, *41*, 576.

(9) Srinivasan, R.; Leigh, W. J. *J. Am. Chem. Soc.* **1982**, *104*, 6784.

(10) Srinivasan, R. *J. Vac. Sci. Technol. B* **1983**, *Y1*, 923; Srinivasan, R.; Braren B. *J. Polym. Sci. Polym. Chem. Ed.* **1984**, *22*, 2601.

(11) (a) Jellinek, H. H.; Srinivasan, R. *J. Phys. Chem.* **1984**, *88*, 3084. (b) Garrison, B. J.; Srinivasan, R. *Appl. Phys. Lett.* **1984**, *44*, 849. Garrison, B. J.; Srinivasan, R. *J. Appl. Phys.* **1985**, *57*, 2909.

(12) Trokel, S. L.; Srinivasan, R.; Braren, B. *Am. J. Ophthalmol.* **1983**, *96*, 710.

0022-3654/86/2090-2124$01.50/0 © 1986 American Chemical Society